Radial and solar cycle variations of the magnetic fields in the heliosheath: Voyager 1 observations from 2005 to 2008

L. F. Burlaga,[1] N. F. Ness,[2] M. H. Acuña,[3] Y.-M. Wang,[4] and N. R. Sheeley Jr.[4]

Received 13 January 2009; revised 23 March 2009; accepted 31 March 2009; published 26 June 2009.

[1] We discuss the magnetic field strength B(t) and polarity observed by Voyager 1 (V1) in the heliosheath at the heliographic latitude ≈34° as it moved away from the Sun from 2005 through 2008.82 (where 2008.0 is the beginning of 1 January 2008). The pattern of the polarity of the magnetic field changed from alternating positive and negative polarities to predominantly negative polarities (magnetic fields pointing along the Archimedean spiral field angle toward the Sun) at ≈2006.23). This transition indicates that the latitudinal extent of the heliospheric current sheet (HCS) was decreasing in the supersonic solar wind, as expected for the declining phase of the solar cycle, and as predicted by extrapolation of the magnetic neutral line near the photosphere to the position of V1. However, the polarity was not uniformly negative in during 2008, in contrast to the predicted polarity. This difference suggests that the maximum latitudinal extent of the HCS was tending to increase in the northern hemisphere in the heliosheath, while it was decreasing in the supersonic solar wind. The large-scale magnetic field strength B(t) was observed by V1 from 2005 through 2008.82. During this interval of decreasing solar activity toward solar minimum, B(t) at 1 AU was decreasing, and the solar wind speed V at the latitude of V1 was increasing. Adjusting the temporal profile of B(t) observed by V1 for the solar cycle variations of B and V in the supersonic solar wind, we find that the radial gradient of B(R) in heliosheath from the radial distance R = 94.2 AU to 107.9 AU between 2005.0 and 2008.82 was 0.0017 nT/AU $\leq$ grad B $\leq$ 0.0055 nT/AU, or grad B = (0.0036 ± 0.0019) nT/AU.

Citation: Burlaga, L. F., N. F. Ness, M. H. Acuña, Y.-M. Wang, and N. R. Sheeley Jr. (2009), Radial and solar cycle variations of the magnetic fields in the heliosheath: Voyager 1 observations from 2005 to 2008, *J. Geophys. Res.*, *114*, A06106, doi:10.1029/2009JA014071.

1. Introduction

[2] Voyager 1 (V1) crossed the termination shock (TS) from the solar wind to the heliosheath on 16 ± 1 December 2004, the uncertainty being due to a data gap [*Stone et al.*, 2005; *Gurnett and Kurth*, 2005; *Decker et al.*, 2005; *Burlaga et al.*, 2005], and V1 has been moving through the heliosheath since that time. Section 2 shows that the magnetometer on V1 [*Behannon et al.*, 1977] observed a decrease in the magnetic field strength B(t) in the heliosheath from 2005.0 to 2008.82 (where 2008.0 is the beginning of 1 January 2008), which was not expected. Voyager 1 observed the transition from alternating positive and negative magnetic polarities to an extended period of negative magnetic polarity beginning at ≈2006.23 and continuing for the next 70 days [*Burlaga et al.*, 2007]. *Burlaga et al.* [2007] suggested that this change occurred because V1 was entering the region of negative polarity of the northern polar magnetic fields as solar activity was decreasing toward solar minimum. We confirm this hypothesis in section 3 by showing that V1 observed predominantly negative polarity from 2006.23 to 2008.2. Using solar observations of the latitudinal extent of the heliospheric current sheet (HCS), we show that the change in the polarity pattern at V1 was caused by the motion of the HCS to below the latitude of V1 (33.6°N) at ≈2006.23. However, we find that the polarity was not uniformly negative after 2006.3. Voyager 1 observed extended intervals of positive polarity during 2008, indicating that the maximum latitudinal extent of the HCS was increasing in the heliosheath to values greater than predicted by extrapolation of the neutral line near the Sun.

[3] The decreasing B(t) observed in the heliosheath by V1 from 2005.0 to 2008.82 as it moved away from the Sun is surprising, since the available models predict an increase in B with increasing distance in heliosheath, as the solar wind slows down when it approaches the heliopause [*Axford*, 1972; *Nerney et al.*, 1991, 1993; *Pauls and Zank*, 1997]. Section 4 shows that there were large solar cycle variations of the supersonic solar wind speed V at the

[1]Laboratory for Geospace Physics, NASA Goddard Space Flight Center, Greenbelt, Maryland, USA.
[2]Institute for Astrophysics and Computational Sciences, Catholic University of America, Washington, D. C., USA.
[3]Planetary Magnetospheres Laboratory, NASA Goddard Space Flight Center, Greenbelt, Maryland, USA.
[4]E. O. Hubert Center for Space Research, Naval Research Laboratory, Washington, D. C., USA.

Copyright 2009 by the American Geophysical Union.
0148-0227/09/2009JA014071

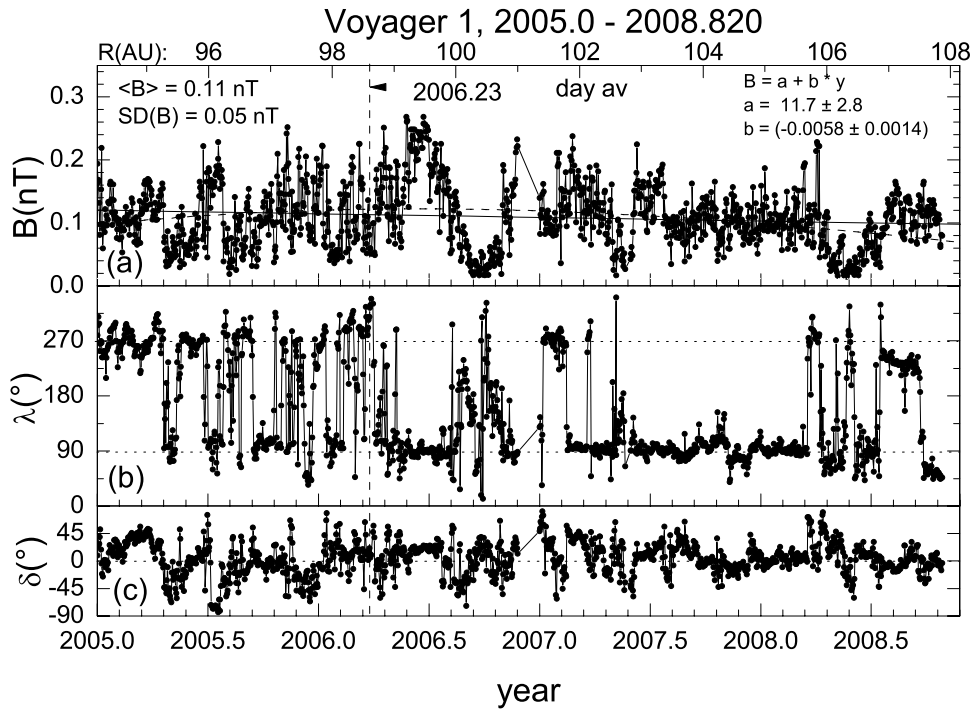

Figure 1. Voyager 1 observations of daily averages of (a) B, (b) the azimuthal angle λ, and (c) elevation angle δ.

latitude of V1 and of magnetic field strength at 1 AU from 2003 through 2008. In section 5, by adjusting the V1 observations of B(t) to account for the solar cycle variations, we calculate the radial gradient of B in the heliosheath from 2005.0 to 2008.82 when V1 moved from 94.2 AU to 107.9 AU and from 34.1°N to 34.3°N.

2. Magnetic Field Observations by Voyager 1

[4] Daily averages of the V1 observations of B, the azimuthal angle λ, and elevation angle δ of the magnetic field from 2005.0 to 2008.82 are shown Figure 1. Data for 37 days (4.1% of the data set) were missing during this interval, mainly owing to gaps in the tracking of the spacecraft. The V1 heliosheath observations from 2005.0 to 2006.9 were presented by *Burlaga et al.* [2007]; the remaining observations in Figure 1 from 2006.9 to 2008.82 are presented here for the first time.

[5] Although the fluctuations in the daily averages of B(t) are very large during much of the time in the interval shown in Figure 1, it is important to determine whether there is a significant change in B as a function of time that might be related to the predicted radial gradient of B(R) in the inner heliosheath.

[6] A linear fit to the data from 2005.0 to 2008.82 gives $B = (11.7 \pm 2.8) - (0.0058 \pm 0.0014)\ y$, which is shown by the solid line in Figure 1a. Thus, the V1 observations indicate a decrease of B with increasing time during the 3.8-year interval in which V1 was moving through the heliosheath toward the heliopause. A cubic fit to the data gives the equation $B = (-0.7 \pm 1.3) \times 10^7 + (10{,}700 \pm 19{,}400)\ y - (5.3 \pm 9.7)\ y^2 - (0.0009 \pm 0.0016)\ y^3$ (where $y \equiv$ year), which is shown by the dashed curve in Figure 1. The cubic fit shows only a small deviation of B relative to the linear fit.

[7] Since V1 was moving ≈3.6 AU/year, it traversed a distance ≈13.7 AU in heliosheath after crossing the TS, which is a sizable fraction of the width of the heliosheath along the direction that V1 is moving (57 ± 2 AU [*Opher et al.*, 2006]; 30–60 AU [*Pogorelov et al.*, 2004]; 79 AU [*Pogorelov et al.*, 2008]; 70–75 AU [*Heerikhuisen et al.*, 2007; *Florinski et al.*, 2009]). The average B during 2005 was 0.11 nT. Estimates of B near the heliopause at the latitude of V1 give B ≈ 0.5 nT. Thus, the models of the heliosheath predict an increase of B with increasing distance from the Sun in the heliosheath. Assuming a linear variation of B with increasing distance in the heliosheath (as a first approximation) one expects a radial gradient of the order of 0.4/79 to 0.4/30 (+0.005 nT/AU to + 0.013 nT/AU, respectively). The predicted positive radial gradient in the heliosheath might appear to be inconsistent with the observed decrease of B(t) as V1 moved toward the heliopause from 2005 through 2008.82. However, the models are based on the assumption that B and the solar wind parameters are constant just upstream of the TS. In sections 3 and 4 we show that this assumption is not valid, since the effects of the solar cycle variation on the B upstream of the TS are significant over the 4-year interval during which V1 was in the heliosheath.

3. Solar Cycle Variation of the Magnetic Field Direction

[8] The heliospheric magnetic field has regions of positive polarity (magnetic field vectors pointing away from the Sun) and negative polarity (magnetic field vectors pointing

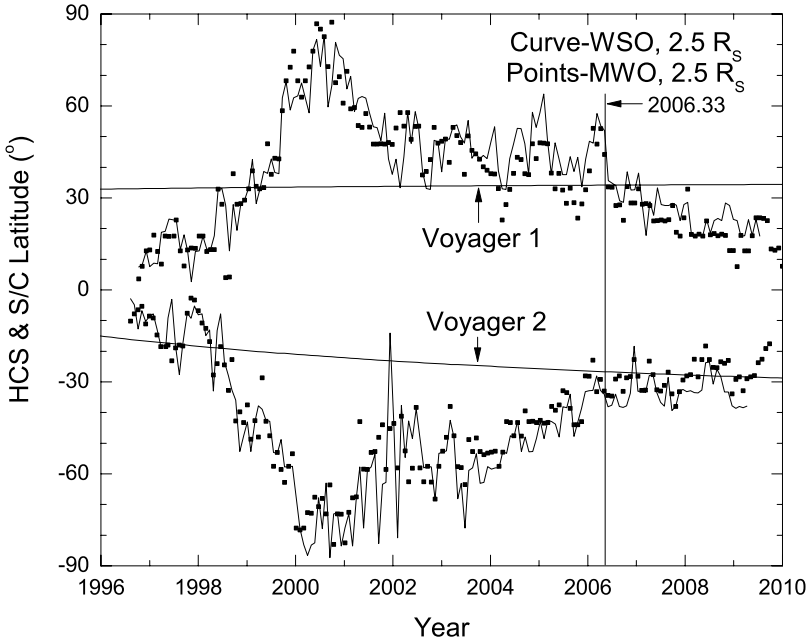

Figure 2. The maximum and minimum of the latitudinal extents of the heliospheric current sheet computed from the "radial model" with a source surface at 2.5 solar radii, with data from the Wilcox Solar Observatory (WSO) and the Mount Wilson Observatory (MWO). The latitudes of V1 and V2 are shown by the nearly straight lines.

toward the Sun) [*Ness and Burlaga*, 2001; *Smith*, 2001]. The idea that the observed sector polarity pattern was related to the existence of a heliospheric current sheet (HCS) was introduced by *Schatten et al.* [1969] and developed by *Schulz* [1973]. During much of the solar cycle, the polarity of the magnetic field is predominantly positive (negative) above the HCS and negative (positive) below the HCS.

[9] A change from alternating positive and negative polarity to a uniform polarity as the HCS moves past a spacecraft toward lower latitudes has been observed by spacecraft <5 AU from the Sun [*Smith et al.*, 1978; *Behannon et al.*, 1989; *Smith et al.*, 1988; *Burlaga and Ness*, 1993; *Balogh and Smith*, 2001]. Evidence for such a transition at $\approx$ 99 AU at $\approx$ 2006.23 was presented by *Burlaga et al.* [2007], who showed that this change in the observed polarity pattern might be related to the decreasing latitudinal extent of the HCS from latitudes greater than that of V1 toward the solar equatorial plane in the supersonic solar wind, as expected during the declining phase of the solar activity cycle.

[10] The sector pattern, which is related to the HCS, is severely distorted with increasing distance from the Sun between 1 AU and 10 AU, owing to dynamical interactions [*Behannon et al.*, 1981]. Nevertheless the maximum latitudinal extent of the HCS changes little, $< O(10°)$, with increasing distance from the Sun out to 40 AU [*Burlaga and Ness*, 1993], and even to $\approx$98 AU as we show below.

[11] Figures 1b and 1c show the direction of **B**, given by the elevation and azimuthal angles δ and λ, respectively, in heliographic coordinates [*Burlaga*, 1995, Figure 2] from 2005.0 to 2008.82. The elevation angle fluctuates about $\delta = 0$. The uncertainties of these angles are large, particularly when B is weak and δ is near +90° and −90°. However, λ shows a change from a bipolar pattern with both positive and negative sectors until 2006.23 to a nearly unipolar pattern with predominantly negative magnetic polarity from the extended interval 2006.23 to 2008.2.

[12] Insofar as the HCS can be approximated as a surface within 1 AU, its intersection with a spherical surface near the Sun is a curve (the "neutral line"). The sphere (the "source surface") was placed at 1.5–2.5 solar radii, and the neutral line was computed from line-of-sight photospheric magnetic field observations using a potential field model by *Schatten et al.* [1969] and *Altschuler and Newkirk* [1969]. Another model, "the radial model", proposed by *Wang and Sheeley* [1992], includes the polar magnetic fields self-consistently. *Burlaga et al.* [1981] found that a correction for the polar magnetic fields was needed in order to explain the polarities observed by Helios.

[13] In this paper we use the maximum and minimum latitudinal extrema of the HCS as a function of time computed using the model of *Wang and Sheeley* [1992] with a source surface at 2.5 solar radii. Figure 2 shows the maximum latitudinal extent of the HCS in the northern and southern hemispheres as a function of time computed with this model using solar magnetic field data from both the Wilcox Solar Observatory (WSO) and the Mount Wilson Observatory (MWO). The data are plotted with a time delay corresponding to the propagation of the solar wind and frozen in magnetic fields at a speed of 400 km/s from the Sun to the positions of V1 and V2.

[14] Figure 2 shows that the radial model predicts that the maximum latitude of the HCS should have dropped below the latitude of V1 at $\approx$2006.33. The sector pattern observed by V1 prior to 2006 is consistent with the predictions of the radial model. A change in the sector pattern was observed by V1 at $\approx$2006.23 (Figure 1b), which is also consistent with the predicted motion of the HCS in the radial model.

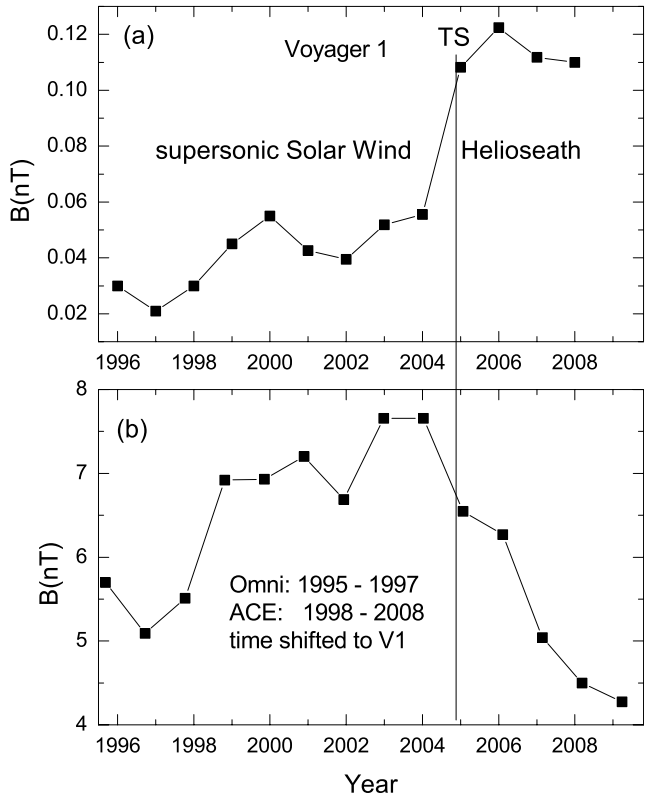

Figure 3. (a) The yearly averages of B measured by V1 as a function of time are shown by the solid squares (connected by straight lines). The vertical line labeled TS is the time that V1 crossed the termination shock from the supersonic solar wind to the heliosheath. (b) The yearly average magnetic field strength at 1 AU as a function of time, projected to the position of V1, is shown by the solid squares (connected by straight lines). The solar cycle variations of B, most evident in the observations near 1 AU, are also observed at V1.

[15] However, V1 observed extensive periods of positive polarity throughout much of 2008 (Figure 1), which is not consistent with the prediction that V1 would observe only negative polarity throughout 2008 (Figure 2). These V1 observations indicate that the maximum latitudinal extent of the HCS was increasing in the heliosheath, in contrast to the decreasing latitudinal extent of the HCS in supersonic solar wind. The competition of these two motions of the HCS could reintroduce positive magnetic polarity intervals amidst the negative magnetic polarity intervals. An increase in the latitudinal extent of the HCS in the northern heliosheath as a consequence of northward flow was discussed by *Pogorelov et al.* [2007a, 2007b]. Further observations and models are needed to test this hypothesis.

4. Solar Cycle Variations of the Magnetic Field Strength and Solar Wind Speed

[16] Previous studies have shown that B varies significantly with the solar cycle [*King*, 1979, 1981] but not with latitude [*Smith and Balogh*, 1995; *Forsyth et al.*, 1996]. It is also well known that V varies significantly with latitude during the declining phase of the solar cycle, when the HCS approaches the ecliptic [see *Phillips et al.*, 1994, 1995; *Burlaga et al.*, 2007, and references therein]. In order to determine the radial gradient of B in the heliosheath that can be compared with predictions of stationary models, it is necessary to adjust the V1 observations of B(t) for the temporal variations of B and V associated with the declining solar activity during the interval of interest (see section 5). We discuss the relevant observations of the solar cycle variations in section 3.

[17] The magnetic field strength observed by V1 from 1996 to 2008 is compared with B observed at 1 AU (with a time delay corresponding to the propagation time to V1 with a speed of 400 km/s) in Figure 3a and Figure 3b, respectively. Figure 3 includes earlier V1 observations over more limited time intervals in figures published by *Burlaga et al.* [1998, 2002]. The observations at 1 AU, obtained from the Omni data set (http://omniweb.gsfc.nasa.gov/index.html) and the ACE data set (http://www.srl.caltech.edu/ACE/ASC/level2/lvl2DATA_MAG.html), show a distinct solar cycle variation of B. The minimum B at 1 AU projected to the position of V1 is a minimum during 1997, rises to a local maximum in ≈2001, rises further to the global maximum in 2003/2004, and then declines monotonically from 2004 to a local minimum in 2009. The corresponding variation of B at V1 is similar. B has a local minimum in 1997, rises to a local maximum in 2000, and then rises to another local maximum in 2004. Voyager 1 crossed the termination shock in December 2004, entering the heliosheath in which B is relatively strong owing to compression by the TS shock.

[18] As we have shown in Figure 1, the large-scale temporal change of B observed by V1 in the inner heliosheath from 2005 through 2008.82 decreased with increasing time, in contrast to the increase of B with time predicted by the stationary models of the heliosheath. Figure 3b suggests a possible explanation for this apparent discrepancy. The B observed at 1 AU shows a decrease from ≈6.5 nT in 2005 to ≈4.5 in 2009, a decrease of 31%. In the absence of other effects, one would expect to observe a similar decrease of B at the position of V1 in the absence of a TS and heliosheath. To zeroth approximation, the decrease of B upstream of the TS with declining solar activity tends to offset the predicted increase of B in the heliosheath with increasing time related to the radial gradient of B and the radial motion of V1.

[19] A determination of the radial gradient of B in the heliosheath from the temporal observations B(t) requires a computation of B at the position of V1 that includes (1) the solar cycle variation of B discussed above and (2) the increase of the speed of the supersonic solar wind associated with the movement of the HCS below the latitude of V1.

[20] The solar wind speed V(t; θ(t), R(t)) varies with time over the course of a solar cycle and with heliospheric latitude θ [see *Burlaga et al.*, 2002, and references therein]. Since V1 moved from the ecliptic at launch in 1977 to ≈34.4°N in 2008, it is necessary to consider the effect of latitudinal variations of the solar wind speed on B at the position of V1, as discussed below. The solar wind speed was not measured in situ at the latitude of V1 after 1980.4, because the plasma instrument on V1 failed. However, *Wang and Sheeley* [1990] and *Sheeley et al.* [1991] showed that the solar wind speed at 1 AU is inversely correlated

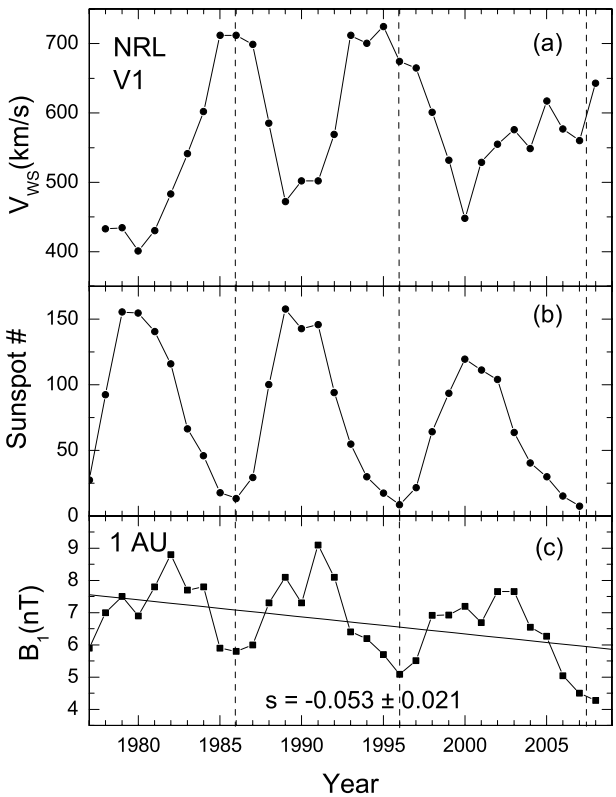

Figure 4. (a) The solar wind speed at V1 as a function of time, computed using the method developed and described in the text, projected to the radial distance of V1. (b) The sunspot number as a function of time for the last three solar cycles. (c) B measured at 1 AU in the ecliptic plane as a function of time for the last three solar cycles.

with the flux tube divergence rate in the corona [*Levine et al.*, 1977]. Thus, it is possible to estimate the solar wind speed at the latitude of V1 from measurements of the photospheric magnetic field, as described by *Burlaga et al.* [2002, Appendix B].

[21] The solar wind speed V(t; θ, R) at the position of V1 computed in this way is shown in Figure 4a. The propagation time of the solar wind moving at constant speed from the Sun to the position of V1 ($\approx$1 year during 2008) is considered in Figure 4a. (The $\approx$20% deceleration of the solar wind produced by the interaction of the solar wind with the neutral interstellar particles that propagate into the heliosphere [*Richardson et al.*, 1995], is small compared to solar cycle variations of this speed, and it can be ignored to first approximation in calculating the propagation time for yearly averages of V.) There is a large solar cycle variation of V(t; θ, R), which is associated with the solar cycle variations of the latitudinal position of the HCS. The solar wind speed is low near the HCS and high in the flows from solar coronal holes at latitudes above the HCS. Figure 4a shows that, in general, the solar wind speed is relatively low (400–500 km/s) at V1 near solar maximum, and relatively high ($\approx$700 km/s) approaching the minimum of the solar cycle (which is shown in the plot of sunspot number versus time in Figure 4b).

[22] The heliospheric magnetic field strength at 1 AU, B_1, varies with the solar cycle (Figure 4c). The magnetic field strength has a minimum at the minimum of solar activity and it has a maximum around the time of the maximum sunspot number. At the current solar minimum, B_1 is exceptionally low, $\approx$4.3 nT, given by data from ACE, WIND, and STEREO available from the NSSDC. This low B is evident in Figure 4c, which shows the variation of B at 1 AU for three solar cycles beginning in mid-1977 with the launch of V1. The maximum magnetic field strength during solar cycle 23 is also low compared to that of two previous cycles. The maximum sunspot number during cycle 23 is also relatively low compared to that during the two previous solar cycles (Figure 4b). The linear fit to B_1(t) in Figure 4c shows an overall decline of B_1(t) during the last three solar cycles. The computed speed at V1 (Figure 4a) at the minimum of solar cycle 23 is also significantly lower than that at the minimum of each of the two previous solar cycles.

5. Radial Variations of the Magnetic Field Strength

5.1. Parker's Model of Radial Variations of the Magnetic Field Strength

[23] Given the information about the solar cycle variations of B and V during the Voyager mission presented above, we can calculate B expected at the position of V1 as a function of time along its trajectory. Following *Burlaga et al.* [1998, 2002] we calculate B at the position of V1 using Parker's spiral magnetic field model [*Parker*, 1958, 1963].

[24] A magnetic field line at a heliographic latitude θ has the form of a spiral wrapped on a cone whose axis is the solar rotation axis and whose angular half-width is $90° - \theta$. According to Parker's model, the strength of the magnetic field in the supersonic solar wind varies as

$$B_p(R, t, \theta) = B_{r1}(t, \theta) R^{-2} \{1 + [419.5R \cos(\theta)/V(t, \theta)]^2\}^{1/2} \quad (1)$$

where the rotation period of the Sun is chosen as $\Omega = 26$ days, independent of latitude. The units of θ, V, and R are degrees, km/s, and AU, respectively. Here B_{r1}(t, θ) is the radial component of the magnetic field at 1 AU and V(t, θ) is the solar wind speed. The time is measured in years; B_{r1}(t, θ) and V(t, θ) are yearly averages. Thus, (1) describes a series of states of the solar wind, rather than a continuous variation of B_p. The functions B_p and V refer to values at the position of the spacecraft. Some care is required when using V determined from solar observations, as discussed below. The first term in the brackets on the RHS of (1) is from the radial component of the magnetic field, which decreases as R^{-2}; the second term is from the tangential component of **B**, which varies as R^{-1}.

[25] The radial component of the magnetic field B_r was shown to be independent of latitude from the heliographic equator to 80° during the first latitude scan of Ulysses as discussed above. A similar result was found in the Ulysses data at solar maximum [*Balogh and Smith*, 2001]. These results suggest that the source magnetic field strength in Parker's model is effectively independent of latitude. Therefore, we assume that there is no latitude dependence in the source term at all phases of the solar cycle, i.e., we take $B_{r1}(t, \theta) = B_{r1}(t)$. From (1) with R = 1 AU and $\theta = 0°$ we obtain $B_{r1} = B_1(t)\,\alpha(t)$, where $\alpha(t) \equiv [1 + (419.5/V_1(t))^2]^{-1/2}$. V_1(t)

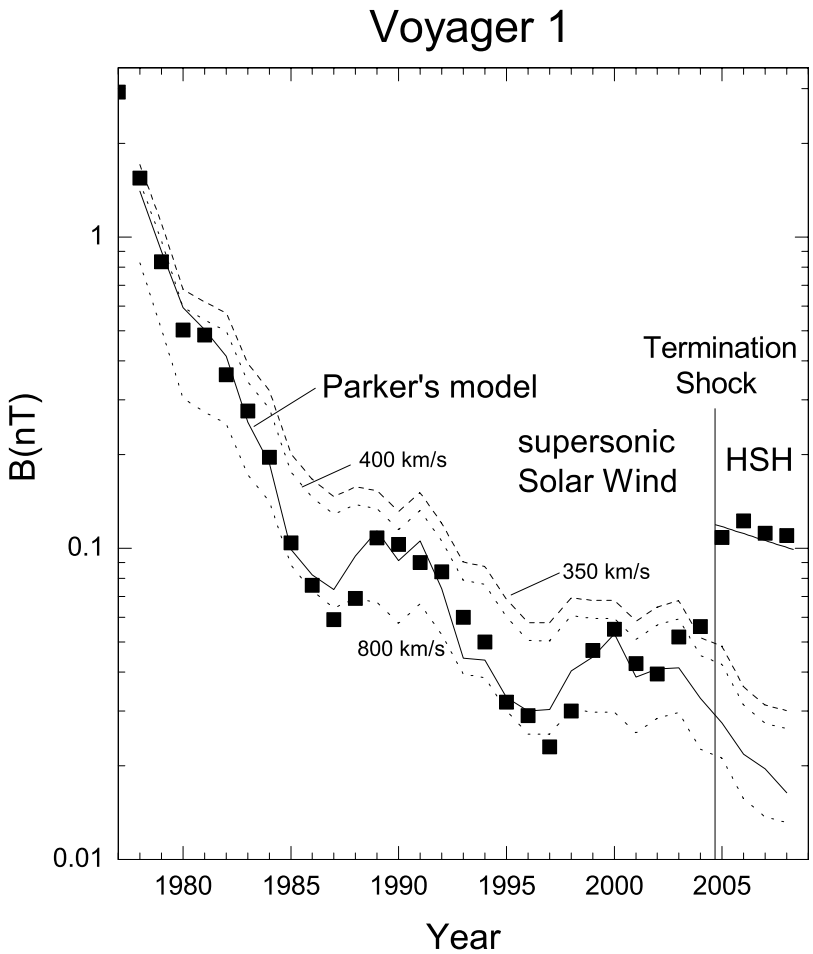

Figure 5. The solid squares show yearly averages of B measured by V1 from 1977 to 2008.82. The solid curve shows B predicted by Parker's spiral magnetic field, with consideration of the solar cycle variations of the solar wind speed and magnetic field strength at 1 AU. The vertical line shows the time that V1 crossed the termination shock from the supersonic solar wind into the heliosheath (HSH).

and $B_1(t)$ are the speed and magnetic field strength, respectively, measured near Earth at 1 AU over the course of a solar cycle. Thus, in the absence of latitude dependence of B_{r1}, Parker's model predicts that along the spacecraft trajectory [R(t), θ(t), φ(t)] equation (1) becomes

$$B_p(R,t,\theta) = \{B_1(t)\left[1+\left(419.5/V_1(t)\right)^2\right]^{-1/2}\}R(t)^{-2} \times \{1+[419.5R(t)\cos(\theta(t))/V(t,\theta(t))]^2\}^{1/2} \quad (2)$$

Note that (2) has no free parameters, since $B_1(t)$, $V_1(t)$ and V(t, θ(t)) can be determined from measurements, as discussed below. Beyond 10 AU, (2) is approximately

$$B_p(t) \sim [(B_1(t)/V(t,\theta(t))] \times R^{-1}\cos(\theta) \quad (3)$$

Equation (3) shows that, in the distant heliosphere, B_p is proportional to B_1 at 1 AU (which varies with the solar cycle) and it is inversely proportional to the solar wind speed (which varies with the solar cycle and the heliographic latitude).

5.2. Comparison of Parker's Model With the Observations of Magnetic Field Strength

[26] This section presents an analysis of new observations of the yearly averages of the V1 data for B(t) from 2001.34 to 2008.82, as well as published results from 1978 to 2001.34. We compare these observations with Parker's model as given by (2).

[27] The observations of B(t) made by V1 from 1978 to 2008.82 are shown as the solid squares in Figure 5. As expected, there is a general tendency for B to decrease with increasing distance from the Sun, which corresponds to increasing time as V1 moves away from the Sun. In addition, however, there are three relative maxima in B near 1980, 1990, and 2000, two relative minima in B during 1987 and 1997, and relatively strong fields from 2005 through 2008. The relatively strong magnetic fields observed after 2004 are heliosheath magnetic fields. Magnetic fields of the solar wind are compressed by the

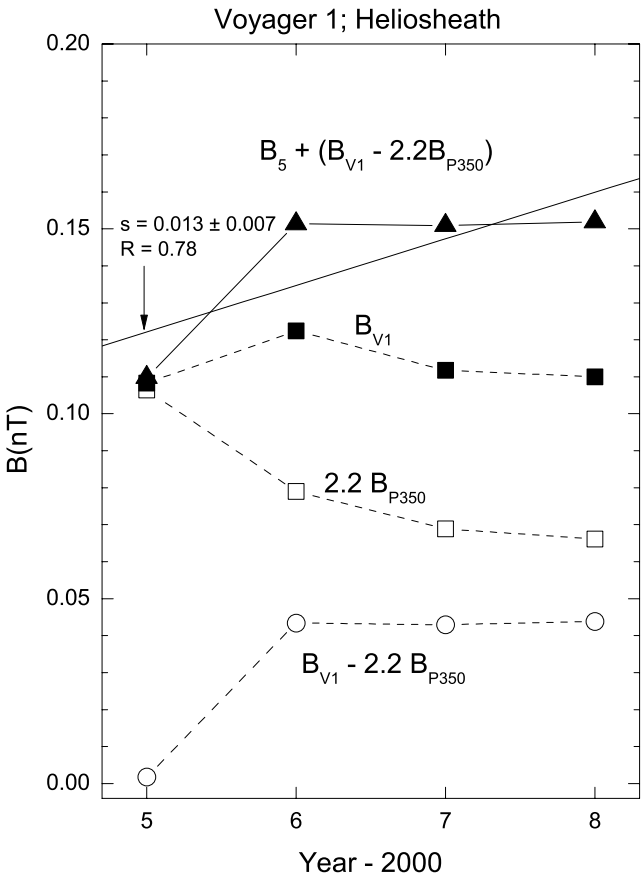

Figure 6. The solid squares show yearly averages of B measured by V1 from 2005.0 to 2008.82. The open squares show B in the heliosheath determined by multiplying B predicted by Parker's model for a speed of 350 km/s (B_{P350}) by 2.2 (the strength of the termination shock in this interval). The open circles show the difference between the observed magnetic field strength in the heliosheath and that predicted by Parker's model. The magnetic field strength in the heliosheath, with the effects of the declining solar activity removed using Parker's model, is shown by the solid triangles.

termination shock as the shock decelerates, compresses, and heats the supersonic solar wind [*Burlaga et al.*, 2005].

[28] The predicted temporal variation of B at V1, based on equation (2) and the curves for $B_1(t)$ and V(t, θ(t)), is shown by the solid curve in Figure 5. The theoretical curve provides a good fit to the observations from 1978 through 2002. As discussed by *Burlaga et al.* [1998, 2002], the relative maxima and minima in B(t) during this interval are related to solar cycle variations in the source field strength (measured by $B_1(t)$) and the solar wind speed at V1, V(t, θ(t)), shown in Figures 4a and 4c, respectively.

[29] The extension of the theoretical curve in Figure 5 to the interval from 2001 through 2008 and the corresponding observations of B in that interval are new results. The predicted magnetic field strengths during 2001 and 2002 are in good agreement with the observed magnetic field strengths.

[30] Equation (2) predicts a decrease of B with increasing distance from the Sun from 2003 through 2008, the declining phase of solar cycle 23, when B_1 was decreasing and V(t, θ(t)) was increasing overall. During 2003 and 2004, the magnetic field strengths observed by V1 in the supersonic solar wind are higher than predicted by Parker's model using V(t, θ(t)) shown in Figure 4a. This anomalously large B could be partly the result of the lower solar wind speeds at larger distances from the Sun, which are produced by the interaction of the solar wind with neutral interstellar particles that penetrate into the heliosphere [*Richardson et al.*, 1995]. Since V1 was approaching the TS [*Decker et al.*, 2008] in 2004, particles propagating upstream from the TS and heliosheath might also tend to reduce the solar wind speed at the position of V1 during 2004, as observed by V2 [*Richardson et al.*, 2008; *Burlaga et al.*, 2008] prior to its crossing of the TS. Parker's model, assuming a low solar wind speed of 400 km/s (shown by the dashed curve labeled 400 in Figure 5) predicts values of B consistent with the observations of V1 in the supersonic solar wind upstream of the termination shock during 2003. Similarly, Parker's model, assuming a solar wind speed of 350 km/s (shown by the dashed curve labeled 350 in Figure 5) predicts values of B consistent with the observations of V1 in the supersonic solar wind upstream of the termination shock from DOY 1 through 350, during 2004.

[31] From DOY 352, 2004 through DOY 215, 2008, V1 was in the heliosheath, where B is relatively strong, as indicated by the observations in Figure 5. The average magnetic field prior to crossing the TS in 2004 was 0.056 nT and the standard deviation was 0.025 nT. The magnetic field strength observed by V1 in the heliosheath behind TS during the year 2005 was $\approx$0.11nT. The ratio of B observed in the heliosheath during 2005 to that observed in the solar wind ahead of the TS during 2004 was $\approx$2.0. The ratio of B observed in the heliosheath during 2005 to that predicted by Parker's model with $\langle V \rangle$ = 350 km/s is equal to 2.2.

[32] Assuming that the average strength of the TS was 2.2 from 2005 through 2008.82, we calculate B in the heliosheath from the magnetic field strength B_{P350} in the solar wind, predicted by Parker's model with an average solar wind speed of 350 km/s. The magnetic field strength in the heliosheath from 2005 through 2008.82 estimated in this way is shown by the open squares in Figure 6, labeled 2.2 B_{P350}. This curve shows that the predicted B in the heliosheath would decrease with increasing time and therefore with increasing distance in heliosheath, if there were no change in the strength and position of the TS and the gradient of B in the heliosheath. This decrease of B_{P350} is a consequence of the decreasing B of the solar wind and the increasing solar wind speed that are associated with the decreasing solar activity. If V1 had crossed the TS during solar maximum, stronger magnetic fields would have been observed in the heliosheath.

[33] The magnetic field strength observed by V1 in the heliosheath from 2006 through 2008.82, shown by the solid squares in Figure 6, is larger than that estimated from Parker's model of the solar wind magnetic field, 2.2 B_{P350} after 2005 by the open squares. The difference between the estimated B = 2.2 B_{P350} and observed B(t) in the heliosheath is shown by the open circles at the bottom of Figure 6, labeled ($B_{V1} - 2.2\ B_{P350}$). If the solar activity had remained constant at the level observed in 2005, then we can estimate that V1 would have observed the magnetic field strengths

shown by the solid triangles in Figure 6, labeled $B_5 + (B_{V1} - 2.2\ B_{P350})$. A linear least squares fit to these data gives a line with a slope of (0.013 ± 0.007) nT/year. Given the speed of V1 relative to the Sun (17.1 km/s = 3.6 AU/year), the slope corresponds to a radial gradient of grad B = (0.0036 ± 0.0019) nT/AU. Thus, by removing the effects of the solar cycle variation on B(t) observed by V1, we can determine the radial gradient of B in the inner heliosheath from 2005 and 2008.82 between 94.2 and 107.9 AU. The result is 0.0017 nT/AU $\leq$ grad B $\leq$ 0.0055 nT/AU.

6. Summary and Conclusions

[34] We analyzed the temporal and radial variation of the magnetic field strength B(t) and polarity observed in heliosheath by V1 from 2005 to 2008.82 as the spacecraft moved from 94.2 AU to 107.9 AU. A linear fit to the observed magnetic field strength B(t) observed by V1 gives a slope −(0.0058 ± 0.0014) nT/year. This negative slope indicates that V1 observed a decrease of B with increasing time during the 3.8 year interval in which it moved a distance of 13.8 AU away from the Sun in the heliosheath.

[35] During the interval under consideration solar activity was decreasing toward solar minimum. The magnetic field strength at 1 AU decreased to the lowest level ever measured by spacecraft. The latitudinal extent of the heliospheric current sheet (HCS) decreased, and there was a corresponding increase in the solar wind speed V. Voyager 1 observed a transition from a pattern of mixed polarity (positive and negative magnetic sectors) to a nearly unipolar pattern at ≈2006.23. The polarity of B after ≈2006.23 was predominantly negative during 2007, corresponding to the polarity of B in the northern hemisphere of the Sun at that time. The transition to the negative polarities observed by V1 in heliosheath was caused by a decrease in the latitudinal extent of the HCS. We arrived at this conclusion by projecting the foot points of the HCS (the neutral line on a source surface of the Sun) radially outward to the position of V1 at the solar wind speed and showing that the HCS moved southward past V1 at the nearly same time that V1 observed a transition to negative magnetic polarity.

[36] During 2008, V1 observed long intervals of positive polarity that were not predicted by projecting the neutral line from the Sun. This observation indicates that the maximum latitudinal extent of the HCS increased in the heliosheath to values greater than predicted by extrapolation of the neutral line on the Sun, while the maximum latitudinal extent of the HCS in the supersonic solar wind was decreasing.

[37] Whereas stationary models of the heliosheath predict that B should increase with increasing distance from the Sun, V1 observed a significant temporal decrease in B during this interval as it moved outward through the heliosheath, in apparent contradiction with the heliosheath models. However, these models assume constant solar wind conditions upstream of the TS, whereas Parker's model, with the appropriate input data that include the effects of declining solar activity, predicts that B(t) observed by V1 in the heliosheath should have decreased with increasing time, which was not observed.

[38] The absence of an increase in B with time at V1 (predicted by the heliosheath models) and the absence of a large decrease in B with time at V1 (predicted by Parker's solar wind model during the declining phase of the solar cycle) can be explained if both effects are significant and tend to balance one another. By adjusting the observed B(t) for the solar cycle effects using Parker's model, we calculate that the radial gradient of the magnetic field in the inner heliosheath was 0.0017 nT/AU $\leq$ grad B $\leq$ 0.0055 nT/AU, or grad B = (0.0036 ± 0.0019) nT/AU, from 2005.0 to 2008.82 between 94.2 AU and 107.9 AU.

[39] The role of the solar cycle variations of the speed and density (and therefore the momentum flux) within a solar cycle must also be considered when modeling the radial gradient of the solar wind speed and density configuration. In particular changes in the momentum flux will change the position of the heliopause and therefore the position of the TS after some time [*Zank*, 1999]. In addition, changes in the solar wind speed and temperature upstream of the TS will modify the position of the TS by changing its rate of convection and its strength [*Whang et al.*, 2003].

Appendix A

[40] In this appendix we use the data set discussed above, which extends to the limit of the supersonic solar wind, in order to confirm two previous results based on smaller data sets: (1) the absence of the "flux deficit" in the supersonic solar wind and (2) a Gaussian distribution of B observed by V1 in the heliosheath.

[41] A quantitative measure of the relative difference between the V1 magnetic field strength observations B_{V1} and the predictions of Parker's model B_p is given by $X(t) \equiv (B_p - B_{V1})/B_p$. *Winterhalter and Smith* [1989] and *Winterhalter et al.* [1988, 1990] suggested that there is a "flux deficit" of 1 − 2.5%/AU in the solar wind beyond 1 AU. *Burlaga et al.* [2002] found no evidence of the "flux deficit" between 1 and 80.5 AU. In particular, they found that the slope of X versus R (the radial distance from the Sun) was s = 0.002 ± 0.005, consistent with 0, with values of X obtained using averages of B measured by V1 from 1978 to 2001.34. Thus, the flux deficit was <0.009%/AU out to 80.5 AU. An extension of the observations of X versus R from 2001.34 to 2004.0, when V1 was at 90.6 AU, is shown by the points in Figure 7. The straight line Figure 7, a linear least squares fit to the observations, has the slope s = 0.0037 ± 0.0041, consistent with 0. The mean value of X is $\langle X \rangle = -0.02 \pm 0.04$, consistent with zero. Thus, observations of B from 1 AU to the TS show no evidence of a "flux deficit". Parker's model describes the variations of B throughout the supersonic solar wind during the last three solar cycles.

[42] Observations of B in the heliosheath by V1 showed that the distributions of daily averages of B are Gaussian, in contrast to the lognormal distributions observed in the solar wind. On the other hand, recent observations of the distribution of B in the heliosheath by V2 [*Burlaga et al.*, 2009] are not consistent with a Gaussian distribution of B. Since the observations of the heliosheath by V2 are very limited, the difference between the distributions observed by V1 and V2 might be a statistical artifact. We must wait for additional observations from V2 in order to obtain a data set of the size comparable to the V1 data set discussed in this paper. But it is of interest to examine the distribution of

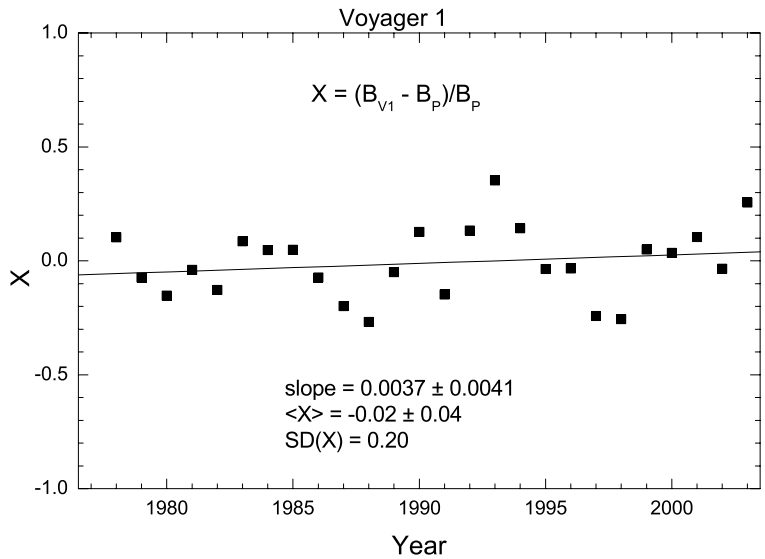

Figure 7. The values of $X \equiv (B_{V1} - B_P)/B_P$ as a function of time. V1 did not observe a "flux deficit" in the supersonic solar wind from 1977 to 2004.0. Parker's model describes B observed by V1 throughout the supersonic solar wind.

daily averages of B measured by V1 for the largest data set available today, from 2005.0 to 2008.82. This distribution, for the 95.9% of the days in the interval for which we have observations, is shown by the points in Figure 8. The solid curve in Figure 8 is a Gaussian fit to the observed distribution, and the dashed curves in Figure 8 are the 95% confidence intervals. In particular, the solid curve is the function $y(\text{days}) = y_0 + \{A/[w \times \sqrt{(\pi/2)}]\} \times \exp[-2 \times (B - B_c)^2/w^2]$,

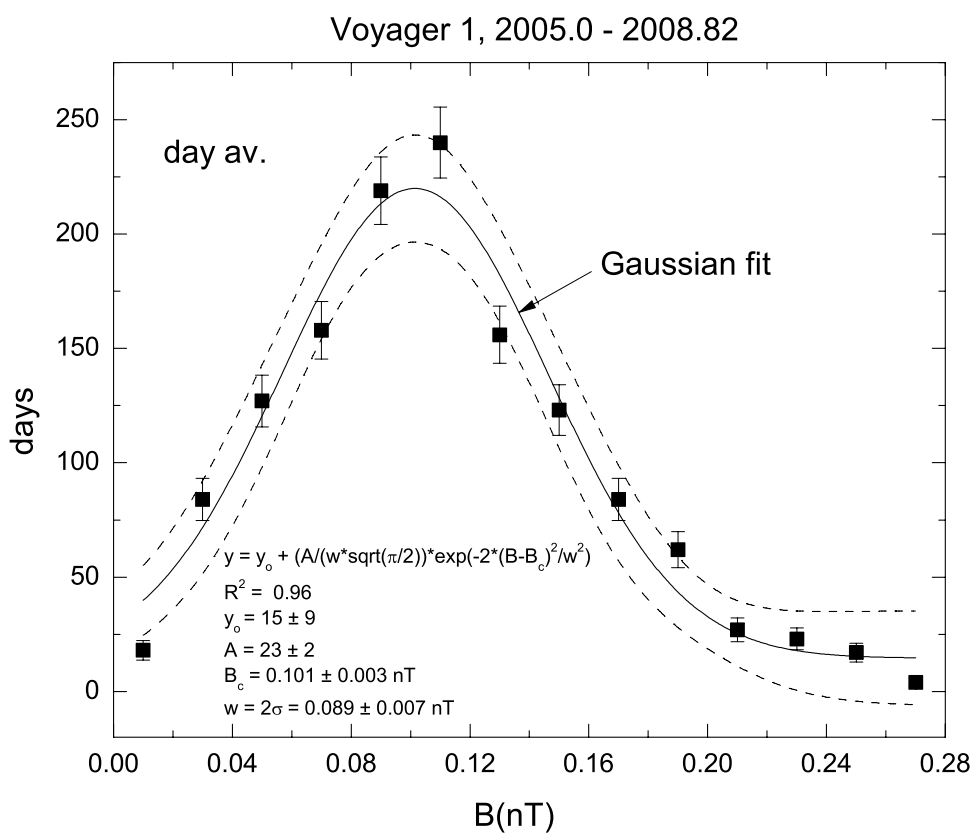

Figure 8. The distribution of daily averages of B observed by V1 in the heliosheath from 2005.0 to 2008.82 (solid curve) and the 95% confidence intervals (dashed curves). The large-scale fluctuations of B in the inner heliosheath have a Gaussian distribution.

where $y_0 = 10 \pm 13$, $A = 24 \pm 3$, $B_c = -0.103 \pm 0.003$ nT, and $w = 2\sigma = 0.098 \pm 0.011$ nT. The coefficient of determination is $R^2 = 0.94$ and all of the points in Figure 8 lie within the 95% confidence interval within their error bars. We conclude that the distribution of daily averages of B in the heliosheath from 2005.0 to 2008.82 is consistent with a Gaussian distribution.

[43] **Acknowledgments.** T. McClanahan and S. Kramer provided help in the processing of the data. Daniel Berdischevsky computed the zero level offsets for the instrument for the data. N. F. Ness was partially supported in part by NASA grant NNX06AG99G to CUA. One of the authors (L.B.) acknowledges helpful conversations with N. Pogorelov.

[44] Wolfgang Baumjohann thanks the reviewers for their assistance in evaluating this paper.

References

Altschuler, M. D., and G. Newkirk Jr. (1969), Magnetic fields and the structure of the solar corona, *Sol. Phys.*, *9*, 131, doi:10.1007/BF00145734.

Axford, W. I. (1972), The interaction of the solar wind with the interstellar medium, *Solar Wind, NASA Spec. Publ.*, *SP-308*, 609–657.

Balogh, A., and E. J. Smith (2001), The heliospheric magnetic field at solar maximum: Ulysses observations, *Space Sci. Rev.*, *97*, 147–160, doi:10.1023/A:1011854901760.

Behannon, K. W., M. H. Acuña, L. F. Burlaga, R. P. Lepping, N. F. Ness, and F. M. Neubauer (1977), Magnetic field experiment for Voyagers 1 and 2, *Space Sci. Rev.*, *21*, 235–257, doi:10.1007/BF00211541.

Behannon, K. W., L. F. Burlaga, J. T. Hoeksema, and L. W. Klein (1989), Spatial variation and evolution of heliosphere sector structure, *J. Geophys. Res.*, *94*, 1245–1260, doi:10.1029/JA094iA02p01245.

Burlaga, L. F. (1995), *Interplanetary Magnetohydrodynamics*, Oxford Univ. Press, New York.

Burlaga, L. F., and N. F. Ness (1993), Large-scale distant heliospheric magnetic field: Voyager 1 and 2 observations from 1986 through 1989, *J. Geophys. Res.*, *98*, 17,451.

Burlaga, L. F., A. J. Hundhausen, and X.-P. Zhao (1981), The coronal and interplanetary current sheet in early 1976, *J. Geophys. Res.*, *86*, 8893–8898, doi:10.1029/JA086iA11p08893.

Burlaga, L. F., N. F. Ness, Y.-M. Wang, and N. R. Sheeley (1998), Heliospheric magnetic field strength out to 66 AU: Voyager 1, 1978–1996, *J. Geophys. Res.*, *103*, 23,727–23,732, doi:10.1029/98JA01433.

Burlaga, L. F., N. F. Ness, Y.-M. Wang, and N. R. Sheeley Jr. (2002), Heliospheric magnetic field strength and polarity from 1 to 81 AU during the ascending phase of solar cycle 23, *J. Geophys. Res.*, *107*(A11), 1410, doi:10.1029/2001JA009217.

Burlaga, L. F., N. F. Ness, M. H. Acuña, R. P. Lepping, J. E. P. Connerney, E. C. Stone, and F. B. McDonald (2005), Crossing the termination shock into the heliosheath: Magnetic fields, *Science*, *309*, 2027–2029, doi:10.1126/science.1117542.

Burlaga, L. F., N. F. Ness, and M. H. Acuña (2007), Magnetic fields in the heliosheath and distant heliosphere: Voyager 1 and 2 observations during 2005 and 2006, *Astrophys. J.*, *668*, 1246–1258, doi:10.1086/521349.

Burlaga, L. F., N. F. Ness, M. H. Acuña, R. P. Lepping, J. E. P. Connerney, and L. D. Richardson (2008), Magnetic fields at the solar wind termination shock, *Nature*, *454*, 75–77, doi:10.1038/nature07029.

Burlaga, L. F., N. F. Ness, and M. H. Acuña (2009), Observations of the heliosheath and solar wind near the termination shock by Voyager 2, *Astrophys. J.*, *692*, 1125–1130, doi:10.1088/0004-637X/692/2/1125.

Decker, R. B., S. M. Krimigis, E. C. Roelof, M. E. Hill, T. P. Armstrong, G. D. Gloeckler, C. Hamilton, and L. J. Lanzerotti (2005), Voyager 1 in the foreshock, termination shock, and heliosheath, *Science*, *309*, 2020–2024, doi:10.1126/science.1117569.

Decker, R. B., S. M. Krimigis, E. C. Roelof, M. E. Hill, T. P. Armstrong, G. D. Gloeckler, C. Hamilton, and L. J. Lanzerotti (2008), Mediation of the solar wind termination shock by non-thermal ions, *Nature*, *454*, 67–70, doi:10.1038/nature07030.

Florinski, V., et al. (2009), The dynamic heliosphere: Outstanding issues, *Space Sci. Rev.*, *143*, 57–83, doi:10.1007/s11214-009-9488-7.

Forsyth, R. J., A. Balogh, T. S. Horbury, G. Erdoes, E. J. Smith, and M. E. Burton (1996), The heliospheric magnetic field at solar minimum: Ulysses observations from pole to pole, *Astron. Astrophys.*, *316*, 287–295.

Gurnett, D. A., and W. S. Kurth (2005), Electron plasma oscillations upstream of the solar wind termination shock, *Science*, *309*, 2025–2027, doi:10.1126/science.1117425.

Heerikhuisen, J., N. Pogorelov, G. Zank, and V. Florinski (2007), The effects of global heliospheric asymmetries on energetic neutral atom sky maps, *Astrophys. J.*, *655*, L53–L56, doi:10.1086/511764.

King, J. (1979), Solar cycle variations in IMF intensity, *J. Geophys. Res.*, *84*, 5983–5940.

King, J. (1981), On the enhancement of the IMF magnitude during 1978–1979, *J. Geophys. Res.*, *86*, 4828–4830.

Levine, R. H., M. D. Altschuler, and J. W. Harvey (1977), Solar sources of the interplanetary magnetic field and solar wind, *J. Geophys. Res.*, *82*, 1061–1065, doi:10.1029/JA082i007p01061.

Nerney, S., et al. (1991), Flow downstream of the heliospheric terminal shock-magnetic-field kinematics, *Astron. Astrophys.*, *250*, 556–564.

Nerney, S., et al. (1993), Flow downstream of the heliospheric terminal shock: The magnetic field on the heliopause, *J. Geophys. Res.*, *98*, 15,169–15,176, doi:10.1029/93JA01177.

Ness, N., and L. F. Burlaga (2001), Spacecraft studies of the interplanetary magnetic field, *J. Geophys. Res.*, *106*, 15,803–15,818, doi:10.1029/2000JA000118.

Opher, M., E. C. Stone, and P. C. Liewer (2006), The effects of a local interstellar magnetic field on Voyager 1 and 2 observations, *Astrophys. J.*, *640*, L71–L74, doi:10.1086/503251.

Parker, E. N. (1958), Dynamics of the interplanetary gas and magnetic fields, *Astrophys. J.*, *128*, 664–676, doi:10.1086/146579.

Parker, E. N. (1963), *Interplanetary Dynamical Processes*, 138 pp., Wiley-Interscience, New York.

Pauls, H. L., and G. Zank (1997), Interaction of a nonuniform solar wind with the local interstellar medium. 2. A 2-fluid model, *J. Geophys. Res.*, *102*, 19,779–19,787, doi:10.1029/97JA01716.

Phillips, J. L., A. Balogh, S. J. Bame, B. E. Goldstein, J. T. Gosling, J. T. Hoeksema, D. J. McComas, M. Neugebauer, N. R. Sheeley Jr., and Y.-M. Wang (1994), Ulysses at 50°S: Constant immersion in the high-speed solar wind, *Geophys. Res. Lett.*, *21*, 1105–1108, doi:10.1029/94GL01065.

Phillips, J. L., et al. (1995), Ulysses solar-wind plasma observations from pole to pole, *Geophys. Res. Lett.*, *22*, 3301–3304, doi:10.1029/95GL03094.

Pogorelov, N. V., G. P. Zank, and T. Ogino (2004), Three-dimensional features of the outer heliosphere due to coupling between the interstellar and interplanetary magnetic fields. I. Magnetohydrodynamic model: Interstellar perspective, *Astrophys. J.*, *614*, 1007, doi:10.1086/423798.

Pogorelov, N. V., et al. (2007a), Unsteady processes in the solar wind interaction with the local interstellar medium, in *Turbulence and Nonlinear Processes in Astrophysical Plasmas: 6th Annual International Astrophysics Conference*, *AIP Conf. Proc.*, *932*, 129–136, doi:10.1063/1.2778955.

Pogorelov, N. V., et al. (2007b), Termination shock asymmetries as seen by the Voyager spacecraft: The role of the interstellar magnetic field and neutral hydrogen, *Astrophys. J.*, *668*(1), 611–624, doi:10.1086/520952.

Pogorelov, N. V., et al. (2008), Probing heliospheric asymmetries with an MHD-kinetic model, *Astrophys. J.*, *675*, L41–L44, doi:10.1086/529547.

Richardson, J. D., et al. (1995), Evidence for a solar-wind slowdown in the outer heliosphere, *Geophys. Res. Lett.*, *22*, 1469–1472, doi:10.1029/95GL01421.

Richardson, J. D., et al. (2008), Cool heliosheath plasma and deceleration of the upstream solar wind at the termination shock, *Nature*, *454*, 63–66, doi:10.1038/nature07024.

Schatten, K. H., J. M. Wilcox, and N. F. Ness (1969), A model of interplanetary and coronal magnetic fields, *Sol. Phys.*, *6*, 442–455, doi:10.1007/BF00146478.

Schulz, M. (1973), Interplanetary sector structure and the heliomagnetic equator, *Astrophys. Space Sci.*, *24*, 371–383, doi:10.1007/BF02637162.

Sheeley, N. R., Jr., E. T. Swanson, and Y.-M. Wang (1991), Out-of-ecliptic tests of the inverse correlation between solar wind speed and coronal expansion factor, *J. Geophys. Res.*, *96*, 13,861–13,868, doi:10.1029/91JA01168.

Smith, E. J. (2001), The heliospheric current sheet, *J. Geophys. Res.*, *106*, 15,819–15,831, doi:10.1029/2000JA000120.

Smith, E. J., and A. Balogh (1995), Ulysses observations of the radial magnetic field, *Geophys. Res. Lett.*, *22*(23), 3317–3320, doi:10.1029/95GL02826.

Smith, E. J., B. J. Tsurutani, and R. L. Rosenberg (1978), Observations of the interplanetary sector structure up to heliographic latitudes of 16°, *J. Geophys. Res.*, *83*, 717–724, doi:10.1029/JA083iA02p00717.

Stone, E. C., et al. (2005), Voyager 1 explores the termination shock region and the heliosheath beyond, September 2005, *Science*, *309*, 2017–2020, doi:10.1126/science.1117684.

Wang, Y.-M., and N. R. Sheeley Jr. (1990), Solar wind speed and coronal flux-tube expansion, *Astrophys. J.*, *355*, 726–732, doi:10.1086/168805.

Wang, Y.-M., and N. R. Sheeley (1992), On potential field models of the solar corona, *Astrophys. J.*, *392*, 310–319, doi:10.1086/171430.

Whang, Y. C., et al. (2003), Solar wind speed and temperature outside 10 AU and the termination shock, *Astrophys. J.*, *589*, 635–643, doi:10.1086/374595.

Winterhalter, D., and E. J. Smith (1989), Observations of large-scale spatial gradients in the heliospheric magnetic field, *Adv. Space Res.*, *9*, 171–175, doi:10.1016/0273-1177(89)90111-7.

Winterhalter, D., E. J. Smith, and J. A. Slavin (1988), The radial gradient in the interplanetary magnetic field between 1 and 23 AU, in *Solar Wind Six*, edited by V. J. Pizzo, T. Holzer, and D. G. Simes, *Tech. Note NCAR/TN-306+Proc*, p. 587, Natl. Cent. for Atmos. Res., Boulder, Colo.

Winterhalter, D., E. J. Smith, and J. A. Slavin (1990), Spatial gradients in the heliospheric magnetic field: Pioneer 11 observations between 1 AU and 24 AU during solar cycle 21, *J. Geophys. Res.*, *95*, 1–11, doi:10.1029/JA095iA01p00001.

Zank, G. P. (1999), Interaction of the solar wind with the local interstellar medium: A theoretical perspective, *Space Sci. Rev.*, *89*(3–4), 413–688, doi:10.1023/A:1005155601277.

M. H. Acuña, Planetary Magnetospheres Laboratory, NASA Goddard Space Flight Center, Code 695, Greenbelt, MD 20771, USA. (mario.h.acuna@nasa.gov)

L. F. Burlaga, Geospace Physics Laboratory, NASA Goddard Space Flight Center, Mail Code 673, Building 21, Room 244, Greenbelt, MD 20771, USA. (burlaga@lepvax.gsfc)

N. F. Ness, Institute for Astrophysics and Computational Sciences, Catholic University of America, Washington, DC 20064, USA. (nfness@bartol.udel.edu)

N. R. Sheeley Jr. and Y.-M. Wang, E. O. Hulburt Center for Space Research, Naval Research Laboratory, Code 7672W, 4555 Overlook Avenue SW, Washington, DC 20375, USA. (neil.sheeley@nrl.navy.mil; yi.wang@nrl.navy.mil)